

Crystal structure of macrophage migration inhibitory factor from human lymphocyte at 2.1 Å resolution

Hiroshi Sugimoto^a, Mamoru Suzuki^b, Atsushi Nakagawa^a, Isao Tanaka^{a,*}, Jun Nishihira^c

^a*Division of Biological Sciences, Graduate School of Science, Hokkaido University, Sapporo 060, Japan*

^b*Photon Factory, National Laboratory for High Energy Physics, Tsukuba 030, Japan*

^c*Central Research Institute, School of Medicine, Hokkaido University, Sapporo 060, Japan*

Received 22 April 1996; revised version received 6 May 1996

Abstract The three-dimensional structure of the macrophage migration inhibitory factor (MIF) from human lymphocytes has been determined by X-ray crystallography at 2.1 Å resolution. The structure was solved by a molecular replacement technique using the coordinates of rat MIF. The molecule forms a trimer structure similar to the rat MIF. However, unlike the rat MIF whose C-terminal tail (residues 104–114) is disordered in the crystal, human MIF has a definite main-chain conformation up to the C-terminal end. These eleven residues create two more β -strands and join to the inter-subunit β -sheet, which contribute to forming a trimer structure. Thus, the trimer structure consists of three seven-stranded β -sheets surrounded by six α -helices. Each β -sheet is comprised of β -strands from each of the three monomers. This architecture is almost identical to 5-carboxymethyl-2-hydroxymuconate isomerase (CHMI) and is related to the *E. coli* signal transducing protein P₁₁.

Key words: Cytokine; Isomerase; Macrophage; X-ray crystal structure

1. Introduction

The macrophage migration inhibitory factor (MIF) was originally identified as a cytokine, derived from T-lymphocytes to prevent the mobilization of guinea-pig macrophages in vitro [1,2]. Further investigation revealed that MIF is secreted from the pituitary and macrophages by lipopolysaccharide (LPS) stimulation, and counter-regulates the immunosuppressive effects of glucocorticoid to act as a critical component of the immunity system [3,4]. Many other properties of MIF, besides its property as an immunoregulatory protein have also been found. MIF exists not only in immune cells, but also in other cell types such as chicken differentiating cells of the eye lens, mouse 3T3 fibroblastic cells and rat liver cells [5–7]. A recent report showed that MIF from the bovine lens has enzyme activity to catalyze the tautomerization of 2-carboxy-2,3-dihydroindole-5,6-quinone (D-dopa-chrome) to 5,6-dihydroxyindole-2-carboxylic acid (DHICA) [8]. Moreover, the three-dimensional structure of MIF from the rat liver has apparent structural similarities with an isomerase [9].

Human MIF is composed of 114 amino acid residues (MW = 12 300) and has 90% amino acid sequence homology to the rat MIF. Although there have been many studies of MIF, little is known about its functions and reaction mechanism in the immunity system. We report here on the crystal

structure of MIF from human lymphocytes determined at 2.1 Å resolution by the method of molecular replacement.

2. Material and methods

Crystals of human MIF were grown by hanging-drop vapor diffusion at 18°C with 2.1 M ammonium sulfate buffered with 100 mM Tris-HCl (pH 8.5). The details of overexpression, purification and crystallization have been described previously [10]. Only the orthorhombic crystal form was used in the present study (space group $P2_12_12_1$ with unit cell parameters $a = 68.4$, $b = 68.8$, $c = 86.8$ Å, three subunits in an asymmetric unit). X-ray intensity data were recorded on an imaging-plate system, DIP-2000K (MAC Science, Japan) using Cu K α radiation. Rotation and translation searches were calculated by XPLOR [11] using the coordinates of the rat MIF trimer produced by the crystallographic three-fold axis [9]. This model includes residues 1 to 103. After the first cycle of simulated annealing refinement, the (2Fo-Fc)-map was calculated, which showed a clear electron density including the C-terminal region (residues 104 to 114), where no density was observed for the rat MIF. At this stage, the electron density map was averaged using the local three-fold axis. The resulting map was sufficiently improved. The model was rebuilt and was subjected to simulated annealing, energy minimization and B-factor refinement in XPLOR. The final R-factor is 22.4%, and free R-factor is 27.1% for all reflections in the resolution range of 8.0–2.1 Å. This model contained 125 water molecules with temperature factor values $B < 50$ Å². All main-chain dihedral angles fall within allowed (91.7%) or additional allowed (8.3%) regions [12] of the Ramachandran plot. The root mean square deviations from ideal bond lengths and angles were 0.011 Å and 1.44°, respectively.

3. Results

Human MIF forms a trimer structure similar to the rat MIF. However, unlike the rat MIF whose C-terminal tail (residues 104–114) is disordered in the crystal, human MIF has a definite main-chain conformation up to the C-terminal end. Fig. 1 shows a MOLSCRIPT [13] schematic diagram for the human MIF monomer. The secondary-structure assignment is given in Fig. 2. The assignment of the secondary structure is almost consistent with the rat MIF C-terminal eleven residues, which were disordered in the crystal of the rat MIF, create two more β -strands and join to the inter-subunit β -sheet, thus contributing to forming a trimer structure, which we describe later in more detail.

The central part of the monomer structure of human MIF consists of a mixed four-stranded β -sheet with two antiparallel helices, which is flanked on one side by one β -strand (β_3 ; residues 46–50) and on the opposite side by two β -strands (β_6 ; residues 105–108, and β_7 ; 111–113). There is a pseudo two-fold axis running perpendicular to the β -sheet in the monomer (Fig. 1). The three monomers are linked together by the hydrogen bonds and create a trimer. Each β -sheet in the trimer is comprised of β -strands from each of the three mono-

*Corresponding author. Fax (81) (11) 746 5232.

E-mail tanaka@polymer.hokudai.ac.jp

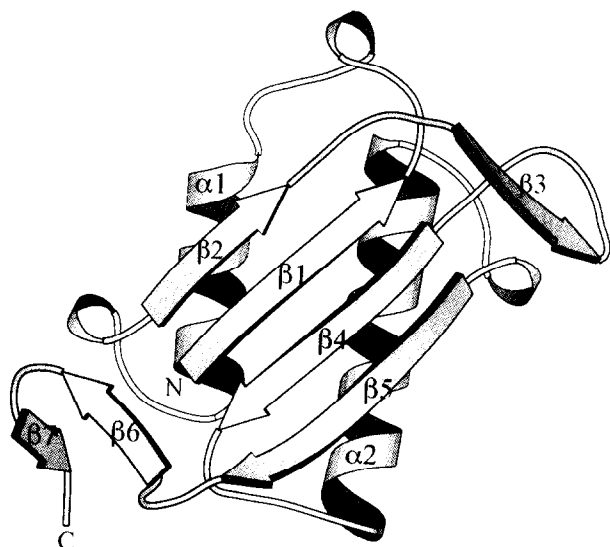


Fig. 1. MOLSCRIPT [13] schematic diagram for the 2.1 Å human MIF monomer. Unlike the rat MIF, whose C-terminal eleven residues are disordered, human MIF has a definite main-chain conformation up to the C-terminal end. These eleven residues create two extra β -strands (strands 6 and 7). The molecule is viewed from a pseudo two-fold rotation axis.

mers. The relationship of secondary structural elements within a trimer is shown in the topological diagram (Fig. 3). With extra β -strands (strands 6 and 7), the molecule forms a more symmetrical trimeric cage-like structure. Thus, the trimer structure consists of three seven-stranded β -sheets surrounded by six α -helices (Fig. 4 top). We call this structure a trimeric β -cage. The overall shape of the MIF trimeric β -cage is cylindrical with approximate dimensions of 54 Å diameter and 38 Å axial length. There is a channel at the center around the

three-fold axis of the trimer. The size of the channel varies from 7 Å to 15 Å, and is large enough for water molecules to pass through. Three subunits are arranged in such a way that a non-crystallographic three-fold axis runs through the center and the pseudo two-fold symmetry axis in a monomer vertically intersects the three-fold axis. Therefore, human MIF trimer exhibits the approximate point group, $D_3(32)$ (Fig. 4 bottom).

In previous studies, MIF has been described as a monomer or dimer [14,15]. However, the fact that the same trimer structure was found in different crystals of proteins from different species strongly suggests that the trimer is the physiologically important structure.

4. Discussion

The structure of the rat MIF has been solved recently, revealing an unexpected similarity to the enzyme 5-carboxymethyl-2-hydroxymuconate isomerase (CHMI) from *E. coli*. CHMI catalyzes the isomerization of 5-carboxymethyl-2-hydroxymuconate (CHM) to 5-carboxymethyl-2-oxo-3-hexene-1,6-dioate (COHED) [16], and has very low sequence homology to the rat MIF (20 out of 126 residues are identical). Both structures consist of three β -sheets surrounded by six α -helices and their topologies in trimer formation are almost identical. The largest differences between these two molecules are in the C-terminal region; C-terminal eleven residues of the rat MIF are disordered in the crystal while they form a β -strand in the CHMI.

Human MIF is more similar to the CHMI than the rat MIF in the overall folding topology of the monomer and trimer. It has two extra β -strands in the region of the C-terminal eleven residues, which were disordered in the rat MIF. In each monomer of human MIF, strand 6 (residues 105–108),

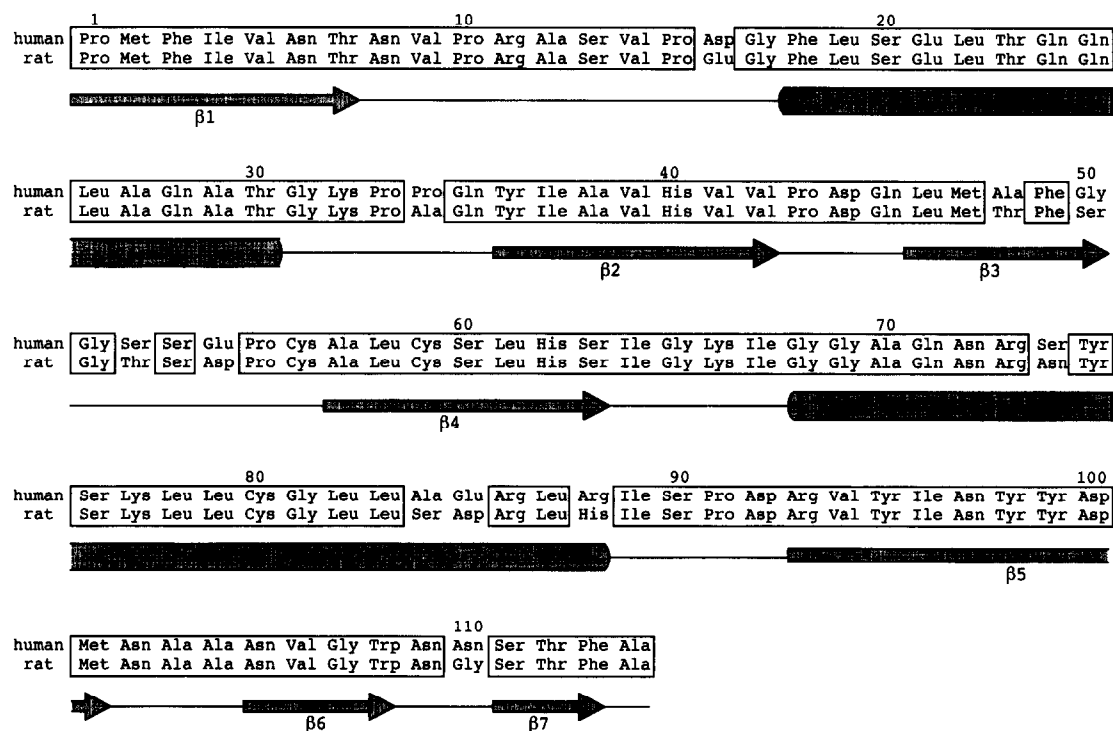


Fig. 2. Sequence alignment of human and rat MIF and the secondary structure assignment for human MIF. The secondary structural elements have been assigned by the inspection of hydrogen bonding and torsion angles.

which is missing in the rat MIF, contributes to the hydrogen bonds with its neighboring monomer in the trimer in a similar way to CHMI. These extra β -strands make the trimer packing more symmetrical and firm. There is, however, another difference between human MIF and CHMI in the secondary structure of the C-terminal region. The C-terminal three residues (111–113) of human MIF which turn back at the β -turn (residues 108–111) make a short seventh β -strand. In contrast, the corresponding region of CHMI is comprised of a 3_{10} helix (residues 121–125) which protrudes into the solvent.

Inspection of amino acid sequences in the C-terminal region revealed only one amino acid difference between the rat and human MIF (Fig. 2). Asn at position 110 is replaced by Gly in the rat MIF. The other different residues do not seem to significantly affect the structure of the C-terminal region. The existence of a small amino acid in this region may endow a peptide chain with a flexible nature, resulting in the disordered structure of the rat MIF. A second possible explanation is that the disordered C-terminal tail of the rat MIF is simply due to crystal packing. The three-fold axis of the human MIF trimer is not a crystallographic one. On the other hand, the three-fold axis of the rat MIF trimer is consistent with a crystallographic one. An exact symmetry may cause the disordered structure in the rat MIF. Whatever the reason is, it is important to note that the C-terminal region does not appear to significantly affect the construction of the trimer structure, and it has some kind of flexibility.

Another protein structure which shows some similarities with MIF is the *E. coli* signal transducing protein P_{II} [1,18]. P_{II} plays a critical role in bacterial nitrogen regulation by controlling the level and activity of glutamine synthetase. This protein also forms a trimer which is comprised of three β -sheets surrounded by six α -helices. However, the monomer structure of P_{II} consists of a central region containing four-stranded antiparallel β -sheet and two antiparallel helices,

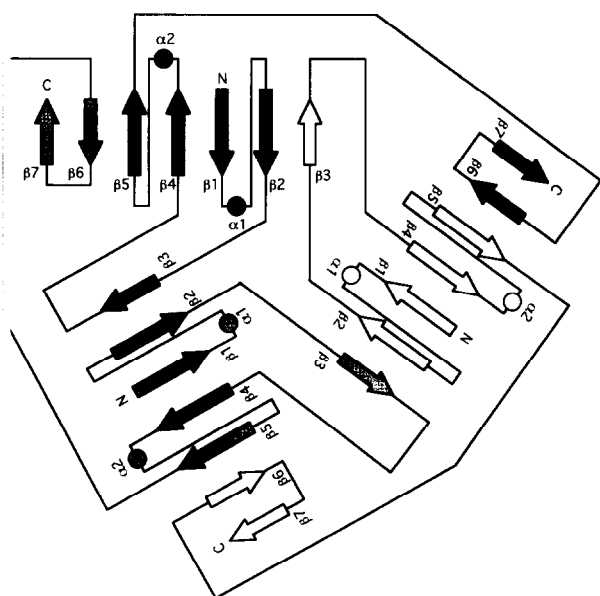


Fig. 3. Topological diagram illustrating the secondary structure elements of human MIF. β -strands are represented by arrows and α -helices by circles. The C-terminal eleven residues, which are disordered in the rat MIF [9], form two more β -strands and join to the β -sheet.

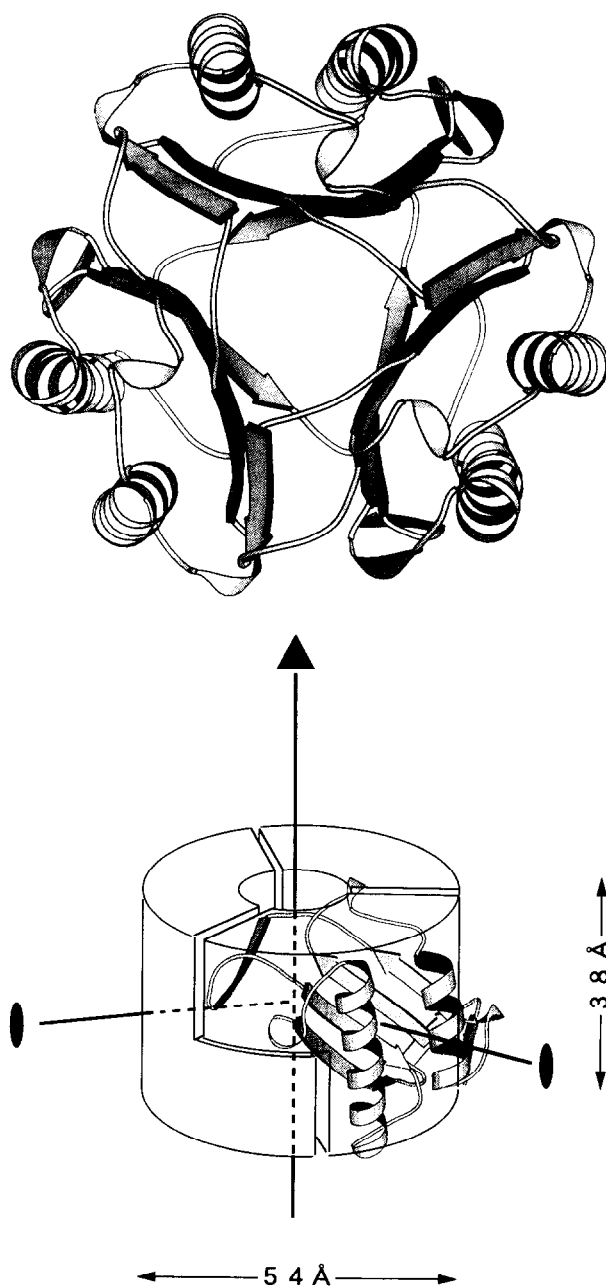


Fig. 4. (top) Trimeric β -cage structure of human MIF viewed from a three-fold axis. (bottom) Schematic representation of human MIF trimer showing pseudo $D_3(32)$ symmetry.

which are connected by intervening loops. Although the folding of the P_{II} monomer is distinct from MIF and CHMI, the way of interactions between each monomer is identical among these molecules. There have been no reports that P_{II} is related to the immune system or isomerase activities. These remarkable structural similarities of two distinct proteins with no sequence homology suggests the importance of β -cage packing, which is characterized by the three central β -sheets and high symmetry with the approximate point group D_3 .

The ideal D_3 symmetry can be formed only by hexameric molecules. This is the case for hexameric 4-oxalocrotonate tautomerase (4-OT). 4-OT catalyzes an analogous reaction to CHMI, and its three dimers, each of which is remarkably similar to the human MIF and CHMI monomer, are arranged

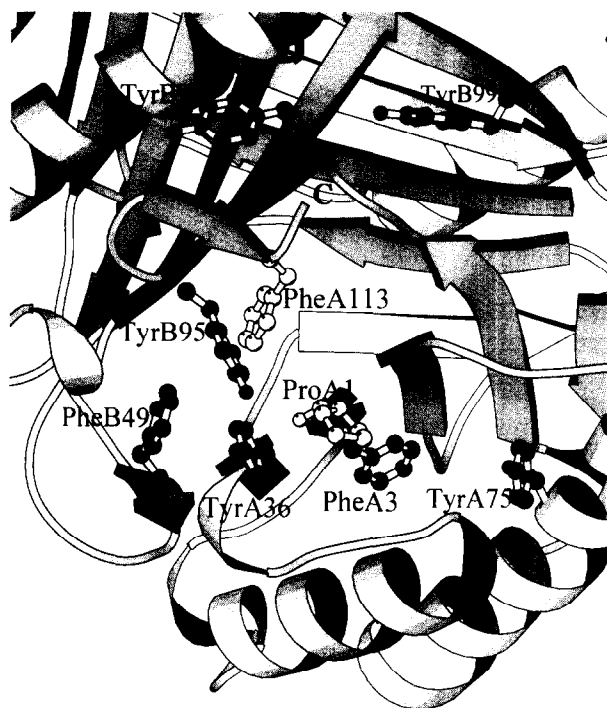


Fig. 5. Proposed catalytic pocket of human MIF in the region close to the N-terminal Pro residue. It is surrounded by aromatic residues. Unlike the C-terminal tail of CHMI, which forms a 3_{10} helix and protrudes in the opposite direction of the active site, the C-terminal β -strand of human MIF participates in a β -sheet and is located near the pocket (especially the side chain of Phe 113).

around the three-fold axis to form a hexamer [19]. The amino acid sequence does not show any similarity with CHMI.

It is proposed that the catalytic base of CHMI is the N-terminal Pro residue which is located in the negatively charged pocket on the molecular surface [19]. On the other hand, although MIF was recently reported to catalyze the tautomerization of 2-carboxy-2,3-dihydroindole-5,6-quinone (D-dopa-chrome) to 5,6-dihydroxyindole-2-carboxylic acid (DHICA) [8], nothing is known about its active site. MIF does have a pocket in a similar region close to the N-terminal Pro residue. However, unlike CHMI, it is surrounded by aromatic residues [9]. The C-terminal 3_{10} helix of CHMI protrudes in the opposite direction to the active site, whereas in the human MIF, the C-terminal β -strand participates in a β -sheet and is located near the pocket (especially the side chain of Phe 113) (Fig. 5). There is no evidence that this pocket is the active site for tautomerization. However, in view of the structural similarity

of the two proteins, it would be rational to speculate that the catalytic sites of the two proteins are in the same region. The flexible nature of the C-terminal tail may effectively be related to the enzymatic activities.

In conclusion, we observed the trimeric β -cage structure in human MIF. A comparison with other β -cage structures suggests that the C-terminal tail has some kind of flexibility. The location of the tail is close to the proposed active site and may be related to the enzymatic activities.

Acknowledgements: This work was supported in part by a grant-in-aid from the Ministry of Education, Science and Culture of Japan.

References

- [1] Bloom, B.R. and Bennett, B. (1966) *Science* 153, 80–82.
- [2] David, J.R. (1966) *Proc. Natl. Acad. Sci. USA* 56, 72–77.
- [3] Bernhagen, J., Calandra, T., Mitchell, R.A., Martin, S.B., Tracey, K.J., Voelter, W., Manogue, K.R., Cerami, A. and Bucala, R. (1993) *Nature* 364, 756–759.
- [4] Calandra, T., Bernhagen, J., Metz, C.N., Spiegel, L.A., Bacher, M., Donnelly, T., Cerami, A. and Bucala, R. (1995) *Nature* 377, 68–71.
- [5] Wistow, G.J., Shaughnessy, M.P., Lee, D.C., Hodin, J. and Zelenka, P.S. (1993) *Proc. Natl. Acad. Sci. USA*, 90, 1272–1275.
- [6] Lanahan, A., Williams, J.B., Sanders, L.K. and Nathans, D. (1992) *Mol. Cell. Biol.* 12, 3919–3929.
- [7] Sakai, M., Nishihira, J., Hibiya, Y., Koyama, Y. and Nishi, S. (1994) *Biochem. Mol. Biol. Int.* 33, 439–446.
- [8] Rosengren, E., Bucala, R., Aman, P., Jacobsson, L., Odh, G., Metz, C.N. and Rorsman, H. (1996) *Mol. Med.* 2, 143–149.
- [9] Suzuki, M., Sugimoto, H., Nakagawa, A., Tanaka, I., Nishihira, J. and Sakai, M. (1996) *Nature Struct. Biol.* 3, 259–266.
- [10] Suzuki, M., Murata, E., Tanaka, I., Nishihira, J. and Sakai, M. (1994) *J. Mol. Biol.* 235, 1141–1143.
- [11] Brünger, A.T. (1993) *XPLOR Version 3.1 Manual*, Yale University, USA.
- [12] Laskowski, R.A., MacArthur, M.W., Moss, D.S. and Thornton, J.M. (1993) *J. Appl. Cryst.* 26, 283–291.
- [13] Kraulis, P.J. (1991) *J. Appl. Cryst.* 24, 946–950.
- [14] Blocki, F.A., Schlievert, P.M. and Wackett, L.P. (1992) *Nature* 360, 269–270.
- [15] Nishihira, J., Kuriyama, T., Sakai, M., Nishi, S., Ohki, S. and Hikichi, K. (1995) *Biochim. Biophys. Acta* 1247, 159–162.
- [16] Hajipour, G., Johnson, W.H., Dauben, P.D., Stolorow, N.J. and Whitman, C.P. (1993) *J. Am. Chem. Soc.* 115, 3533–3542.
- [17] Cheah, E., Carr, P.D., Suffolk, P.M., Vasudevan, S.G., Dixon, N.E. and Ollis, D.L. (1994) *Structure* 2, 981–990.
- [18] Carr, P.D., Cheah, E., Suffolk, P.M., Vasudevan, S.G., Dixon, N.E. and Ollis, D.L. (1996) *Acta Crystallog. sect. D* 52, 93–104.
- [19] Subramanya, H.S., Roper, D.I., Dauter, Z., Dodson, E.J., Davies, G.J., Wilson, K.S. and Wigley, D.B. (1996) *Biochemistry* 35, 792–802.